Wafer fused *p*-InP/*p*-GaAs heterojunctions

F. Salomonsson,[a] K. Streubel, J. Bentell, M. Hammar, D. Keiper, and R. Westphalen
Department of Electronics, The Royal Institute of Technology, Electrum 229, S-164, 40 Kista, Sweden

J. Piprek
University of Delaware, Materials Science Program, 201A Spencer Laboratory, Newark, Delaware 19716-3106

L. Sagalowicz, A. Rudra, and J. Behrend
Institut de Micro et Optoélectronique, Département de Physique, Ecole Polytechnique Fédérale de Lausanne, 1015 Lausanne, Switzerland

(Received 16 June 1997; accepted for publication 13 October 1997)

This article reports on the fabrication and characterization of wafer fused heterojunctions between p-InP and p-GaAs. Secondary ion mass spectroscopy was used to characterize doping profiles across the interface as well as the interface contamination with oxygen or carbon. The crystalline quality of the fused material was characterized using cross section and plan-view transmission electron microscopy. The electrical properties of the fused interface were studied as a function of various doping elements such as Be and Zn in InP or Zn and C in GaAs as well as for different acceptor concentrations in GaAs. Finally, the electrical characteristics were analyzed using a numerical model that includes thermionic emission and tunneling across the heterobarrier. © *1998 American Institute of Physics.* [S0021-8979(98)04002-X]

INTRODUCTION

The technique of wafer fusion is a viable processing tool to combine semiconductor materials independent of their lattice constant. It removes the limitation to lattice matched materials given by epitaxial growth techniques and opens a new degree of freedom for the design of semiconductor devices. In contrast to similar techniques, such as epitaxial lift off or silicon/silicon dioxide bonding, wafer fusion (or ''bonding by atomic rearrangement'') does not involve any foreign material at the interface. Instead, both materials are directly joined together and covalent bonds are formed on either side of the fused interface. The electrical and optical properties of wafer fused heterojunctions are very similar to those of epitaxially grown interfaces. This enabled the fabrication of novel devices such as the silicon heterointerface photodetector,[1,2] wafer fused vertical cavity lasers (VCSELs),[3,4] resonant cavity photodetectors,[5] or transparent substrate light emitting diodes.[6,7]

Wafer fusion has been around for several years and has been applied to a variety of materials. Liau *et al.*[8] were the first to fuse III–V based optoelectronic devices to silicon or GaAs substrates, a technique that has been adopted by many groups.[9–11] The fusion of InP and GaAs has attracted a lot of interest in the recent years because of its very successful use in the fabrication of long wavelength VCSELs.[12,13] Wafer fused GaAs/InP VCSELs benefit from the high index contrast and good thermal properties of AlGaAs/GaAs Bragg mirrors as well as from the high optical quality of InP-based active layers in the 1.3–1.55-μm-wavelength regime. Submilliampere threshold currents and high temperature operation above 100 °C have been demonstrated with double-fused VCSELs.[14] These lasers involve two fused InP/GaAs interfaces inside the optical cavity demonstrating the excellent electrical and optical properties that can be achieved with wafer fusion.

The transport of carriers across the GaAs/InP heterojunction is a major concern for electrically driven, fused VCSELs. A low electrical resistance is essential to reduce heating close to the active region, which would otherwise result in a significant redshift of the optical gain. VCSELs are particularly susceptible to this effect because their performance is critically dependent on the overlap of the optical gain with the single longitudinal cavity mode.[15] Active layer heating also increases the already high nonradiative loss mechanisms at a long wavelength resulting in a high threshold gain and low quantum efficiency.

The electrical properties of InP/GaAs junctions have been characterized previously by $I(V)$ measurements[16] and admittance spectroscopy.[17] Experimental $I-V$ curves of n-InP/n-GaAs interfaces could be described using a simple thermionic emission model.[16] An effective electron barrier, which is closely related to the conduction band discontinuity, could be determined from the measured $I-V$ curves. However, the model failed to describe the experimental $I(V)$ characteristics of the p-InP/p-GaAs junctions. The p-p fused interfaces were found to be highly resistive for hole transport and the experimental results did neither agree with the thermionic emission theory nor the admittance spectroscopy results.

In this work, we focused specifically on the fabrication and characterization of low resistive wafer fused p-InP/p-GaAs heterojunctions. The fused junctions were seen as an integrated part of the electrically driven vertical cavity devices implying the simultaneous optimization of electrical and optical properties. Special attention was devoted to find a trade-off between high acceptor concentrations for improved hole transport and the below-band gap absorption in p-GaAs and p-InP.[18] The crystalline quality of the fused interfaces was analyzed using cross section and

[a]Electronic mail: fredriks@ele.Kth.se

 0021-8979/98/83(2)/768/7/$15.00 © 1998 American Institute of Physics

plan view high resolution transmission electron microscopy (HRTEM). The electrical properties were systematically studied as function of the GaAs hole concentration. $I-V$ curves were measured in a temperature range between $-150\,°C$ and room temperature. Different doping elements for GaAs (Zn and C) and InP (Zn and Be) were compared with special emphasis on the diffusion behavior and its impact on the $I-V$ characteristics. The actual doping profiles after fusion as well as possible interface contamination were characterized by secondary ion mass spectroscopy (SIMS). Finally, a comprehensive model was developed to describe the measured $I-V$ curves. Thermionic emission as well as drift diffusion and tunneling effects were taken into account to describe the experimental results.

EXPERIMENT

For this study, a set of 1-μm-thick Zn and C-doped GaAs layers was grown on (100) exact oriented GaAs:Zn substrates. The doping levels for each element were 1×10^{18}, 5×10^{18}, and 1×10^{19} cm^{-3}. The samples were fused to pieces of the same InP wafer consisting of a 0.3-μm-thick p-InP fusion layer grown on top of a 0.3 μm GaInAs/0.5 μm InP/0.4 μm GaInAs etch stop structure on a (100) oriented InP substrate. The fusion layer was Zn doped to a level of $p=1\times 1018$ cm^{-3}. Additionally, the C-doped GaAs samples were fused to a Be-doped InP sample of otherwise identical structure. The Be-doped sample was grown by chemical beam epitaxy (CBE) at 480 °C, all other samples were grown by low pressure metal organic vapor phase epitaxy (LP-MOVPE) at 680 °C.

Prior to fusion, the samples were cleaved to 10×12-mm-sized pieces in order to mark the original orientation on the wafer. The average surface roughness, measured by atomic force microscopy (AFM) of both materials was typically below 1 nm. An array of 10-μm-wide 0.3-μm-deep channels with a pitch of 150 μm was etched through the InP surface to the first GaInAs etch-stop layer. Such channels have been found to improve the quality of the fused interface by reducing the defect density in terms of voids or bubbles, presumably by enhancing the transport of desorbed gases from the interface.[19] The cleaning procedure for GaAs and InP surfaces started with an oxygen plasma treatment in order to remove hydrocarbons and to create a defined oxide film. Subsequent oxide removal and cleaning was done in a HF:HCl solution followed by NH_4OH. Both samples were brought into contact and aligned in the NH_4OH solution (''wet bonding'') without exposing them to air. The aligned wafers were mounted in a stainless steel fixture applying a pressure of 2×10^6 Pa at room temperature. For the actual fusion process, the samples were heated to 650 °C for 30 min in a H_2 atmosphere.

SIMS and $I(V)$ measurements were performed on the InP side of the fused samples. The InP substrate and the first GaInAs etch-stop layer were removed by selective etching using HCl:H_2O (3:1) and H_3PO_4:H_2O_2:H_2O (1:205:40), respectively. For the electrical characterization, circular mesas with a diameter of 280 μm were etched through the InP/GaInAs/InP structure and the fused junction into the GaAs sample. Two pairs of Au/Zn concentric ring contacts were deposited by electron beam evaporation on top and around the mesas for $I(V)$ measurements in a four probe geometry. The contacts were annealed at 430 °C for 30 s in order to restrict the diffusion of Zn to a few 100 nm.

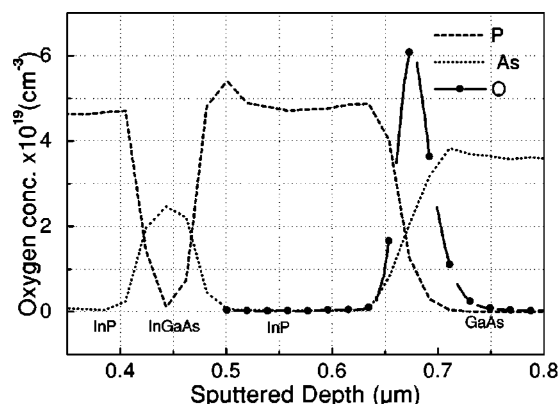

FIG. 1. SIMS analysis across a wafer-fused GaAs:Zn/InP:Zn heterojunction. Solid line: oxygen signal, dashed line: Phosphorous, dotted line arsenic.

SIMS ANALYSIS

In order to extract more information on the chemical nature of the wafer fused interface, the samples were characterized by SIMS. Cesium ions were used for sputtering in order to enable the detection of oxygen atoms. Figure 1 depicts the depths profile of the oxygen concentration of the InP:Zn/GaAs:Zn sample. P and As traces were measured simultaneously to mark the exact position of the fused junction. The measurement shows a clear oxygen signal at the interface. The calibrated oxygen concentration is 6×10^{19} cm^{-3}. Integration over the width of the oxygen peak gives an oxygen area concentration of 2.5×10^{14} cm^{-2}. This is less than the number of atoms in a lattice plane, which confirms the absence of a homogeneous oxide film at the interface.

Next the diffusion of Zn and Be across the fused interfaces was studied. Zn in InP and GaAs is known to diffuse at high temperatures with a concentration dependent diffusion coefficient.[20,21] The typical situation for low resistive wafer fused p-p junctions in electrically driven devices are relatively high doping levels around 1×10^{18} cm^{-3} which are exposed to a high temperature of 400–600 °C for several min. Acceptor diffusion inside both materials and across the interface has to be expected and might even be beneficial for an effective hole transport by reducing the potential barrier in the valence band. The Zn and C profiles across the InP:Zn/GaAs:C ($p=1\times 10^{19}$ cm^{-3}) interface are shown in Fig. 2. The Indium is given as a marker for the different materials involved. The curves clearly show a significant concentration of both Zn and C at the interface. The zinc concentration decreases on the InP side towards GaAs and rises sharply at the fused junction. Similar Zn profiles are measured on the InP:Zn/GaAs:Zn sample. Further diffusion of Zn into the GaAs layer is observed with a Zn concentration of 1×10^{18} cm^{-3} directly behind the heterojunction decreasing by one order of magnitude at a depth of 300 nm in the GaAs layer. The measured Zn profile is the combined result of two

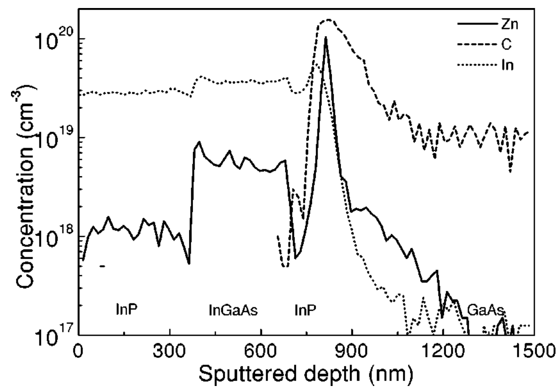

FIG. 2. SIMS analysis of the dopant profiles across the InP:Zn/GaAs:C interface.

effects: (a) possible segregation of Zn at the surface during growth and (b) diffusion during the fusion process. For the high doping levels and high temperatures, the second effect is dominating. It should be noted that the SIMS measurements, by necessity, were performed before the contacts were formed, and thus do not reflect a possible Zn diffusion to the interface from the contacts. However, the application of short annealing times minimizes such diffusion. Earlier SIMS measurements show that this indiffusion is less than two hundred nanometers, which corresponds well with values found in literature.[22]

Carbon has been shown to have a significantly lower atomic diffusion coefficient in GaAs than other p-type dopants.[23,24] The detected high carbon interface levels of 1×10^{20} cm^{-3} is therefore attributed mostly to residual hydrocarbons after surface cleaning or contamination during the fusion process itself.

Be in GaAs is a slowly diffusing impurity except for the highest concentrations.[25] Be in GaP shows a small diffusion length, but a strong redistribution at higher concentrations.[26] Very little has been reported on the diffusion behavior of Be in InP,[27] but it seems reasonable to assume that it is lower than for Zn also in this material. Figure 3 shows the Be profile in the InP:Be/GaAs:C, $p=1\times10^{19}$ cm^{-3} together with the As and P signals throughout the entire structure including the GaInAs etch-stop layer. Be shows a clear tendency to diffuse and accumulate at the fused interface as well as at the epitaxial InP/GaInAs interfaces. The Be signal at

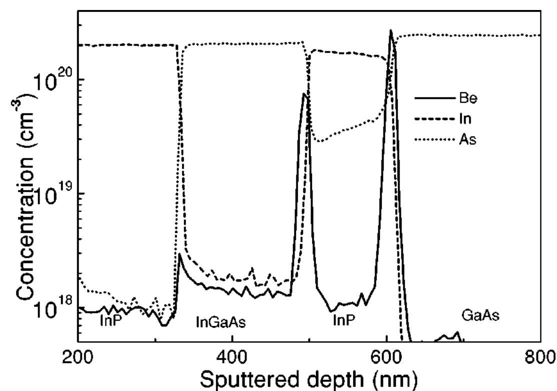

FIG. 3. SIMS profiles of Be, As, and In across the InP:Be/GaAs:C interface.

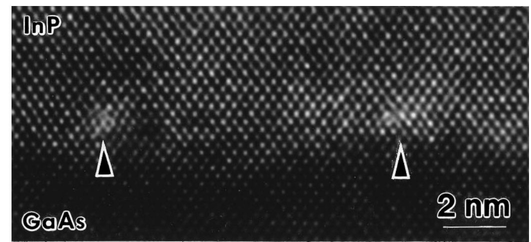

FIG. 4. HRTEM the interface (cross section).

the fused interface is about two orders of magnitude larger than the bulk concentration, which is comparable to the accumulation of Zn. However, SIMS measurements on different spots on the wafer showed some lateral variations of the Be concentration which make a direct comparison between the behavior of Zn and Be difficult. The origin of the Be accumulation at the fused interface could also be due to segregation during growth, however it has been shown[28] that for CBE this is only a problem for high growth temperatures.

TEM ANALYSIS

Figure 4 shows a [110] HRTEM image of the interface. It is observed that the interface is constituted of perfect regions separated by dislocations (arrowed). The projection of the Burgers vector is 1/2[1−10]. The average spacing between the interfacial dislocations is about 10 nm as it is necessary to relax the 3.7% misfit between InP and GaAs.

Figure 5(a) is a plan-view image which was obtained using the (2−20) reflection and weak beam conditions. One set of dislocations is visible. Another set is visible in the (220), (400), and (040) reflections. The angle between the two sets is 90°, and the network is schematicly represented in

(a)

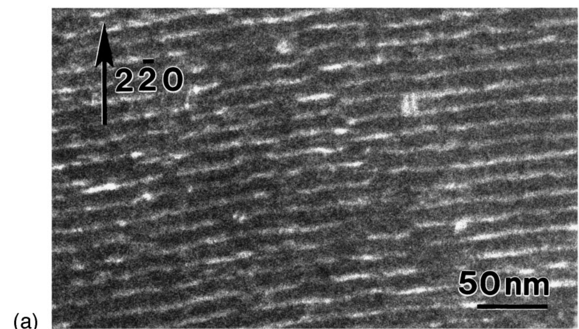

[110]
$[1\bar{1}0]$
1
η
2 2 2 2
1
1
1

(b)

FIG. 5. Plan-view image of the interface. (a) (2−20) weak beam image. (b) Schematic of the dislocations network. The Burgers vector of the dislocations composing set 1 is 1/2[1−10] and of set 2 is 1/2[110].

Fig. 5(b). The spacing between the dislocations is close to 10 nm. Those dislocations are not exactly edge dislocations. Their line lies at about 10° from [110] and the angle between their line direction and the Burgers vector is 80°. The selected area diffraction pattern indicates that a twist angle of about 0.5° is present. It is usually assumed that wafer fusion between InP and GaAs substrates will produce edge dislocations. However this is not exactly the case when a twist angle even small is present. The geometry of the dislocation network when a twist is present can be understood. It is well known that the mismatch of an epitaxial (001) interface between two face cubic centered (fcc) crystals having different lattice parameters is accommodated by a square network of edge dislocations. It is also known that the misorientation of a (001) twist boundary in fcc is accommodated by a square network of screw dislocations. In both cases, the Burgers vector of the dislocations composing the network are $1/2[110]$ and $1/2[1\bar{1}0]$. Therefore the misfit (lattice mismatch) twist interface will be composed of dislocations having Burgers vectors $1/2[110]$ and $1/2[1\bar{1}0]$ and having line direction of the dislocations will be rotated of an angle η from a pure misfit boundary [Fig. 5(b)]. Clearly η increases as the twist angle increases. The precised description of the geometry of the dislocation network in function of the misorientation between the two wafers as well as the complete interpretation of the plan-view TEM image is given somewhere else.[29]

ELECTRICAL CHARACTERIZATION

The realization of p-GaAs/p-InP heterojunctions with high optical and electrical quality is one of the most critical processing steps in the fabrication of wafer-fused VCSELs. Contrary to n-n junctions, the carrier transport across p-p junctions appears to be of high resistance and the measured $I-V$ curves can not be described with simple thermionic emission theory. So far, the cause for the high hole resistance is not known, but it is suspected, that it is related to interface dislocations or contamination. The motivation for this work was primarily to reduce the voltage drops at the wafer fused p-p interface and to understand the transport mechanism across the heterojunction.

The current–voltage characteristics of fused heterointerfaces have been measured between two contacts on the InP mesas and two concentric contacts on the GaAs surface around the mesas. The inner and outer contacts were connected to a current source while the resulting voltage drop was measured on the contacts between. In this geometry, the contact resistance, which is of the same order of magnitude as the junction resistance here will be excluded. The InP side was biased positive with respect to GaAs, which is referred to as forward biasing.

The $I-V$ curves for three different combinations of dopants are shown in Fig. 6. Good electrical conductance under forward and reverse bias has been obtained in all three cases. In fact, the voltage drops are the lowest ever reported for wafer fused p-GaAs/p-InP heterojunctions. Zn and C-doped GaAs gave the same low voltage drops under forward bias when fused to Zn-doped InP, whereas somewhat higher values were obtained with the InP:Be sample [Fig. 6(c)]. Also under reverse bias, the InP:Be/GaAs:C sample showed the highest voltage drops, while both GaAs samples fused to InP:Zn gave lower values. The cause for the high voltage drops obtained with the InP:Be sample could be related to a different diffusion behavior of Be in InP compared to Zn. However, it appears to be more likely that the low growth temperature in CBE, which has been used for this particular sample, is responsible for the difference to the MOVPE grown samples. At growth temperatures as low as 480 °C,

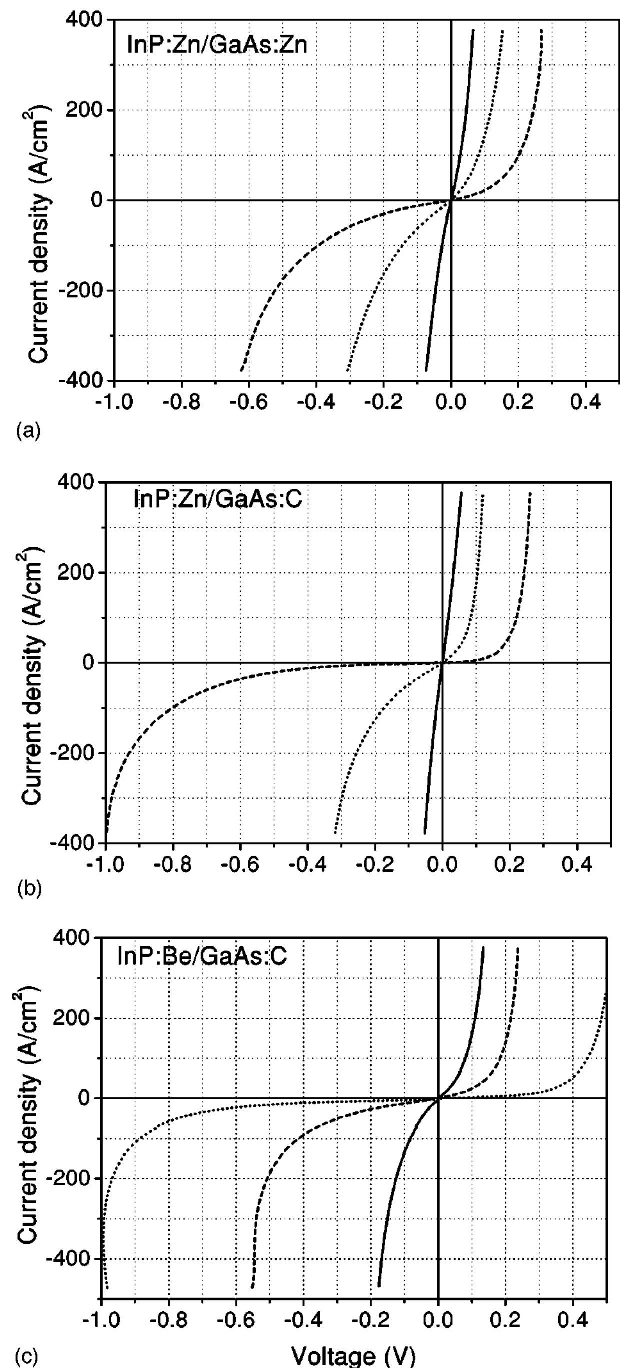

FIG. 6. Current–voltage characteristics at room temperature at three different doping levels in GaAs: $p=1\times 18\ cm^{-3}$ (solid line), $p=5\times 18\ cm^{-3}$ (dashed line), $p=1\times 19\ cm^{-3}$ (dotted line), (a) InP:Zn/GaAs:Zn, (b) InP:Zn/GaAs:C, and (c) InP:Be/GaAs:C.

the surface mobility of the growing species is low, which can affect the crystalline quality of the grown layer, e.g., by the incorporation of point defects. Other groups have observed that epitaxial layers grown under comparable conditions showed a blue shift in photoluminescence after wafer fusion.[30]

The solid, dashed, and dotted lines in Figs. 6(a)–6(c) show the impact of the doping level on the $I-V$ characteristics. Independent of the dopant species, the lowest voltage drops are obtained with the lowest GaAs hole concentration of 1×10^{18} cm^{-3} (solid lines). Increasing the doping level to 5×10^{18} cm^{-3} (dashed lines) resulted in a significantly higher voltage drop under forward and, even more pronounced, under reverse bias. At the highest doping level of 1×10^{19} cm^{-3} (dotted lines), the voltage drops reduced again for the InP:Zn samples without reaching the low values of the lowest doped samples. Here again, the InP:Be sample behaved differently, although a systematic tendency was difficult to see because of large fluctuations over this particular sample. The varying results are merely attributed to lateral fluctuations in the epitaxial layer rather than an inhomogeneous wafer fusion. Figure 7 depicts the same series of $I-V$ curves measured in a temperature range of 150–350 K. All samples showed the same exponential temperature dependence indicating no obvious differences in the carrier transport mechanism across the fused junctions.

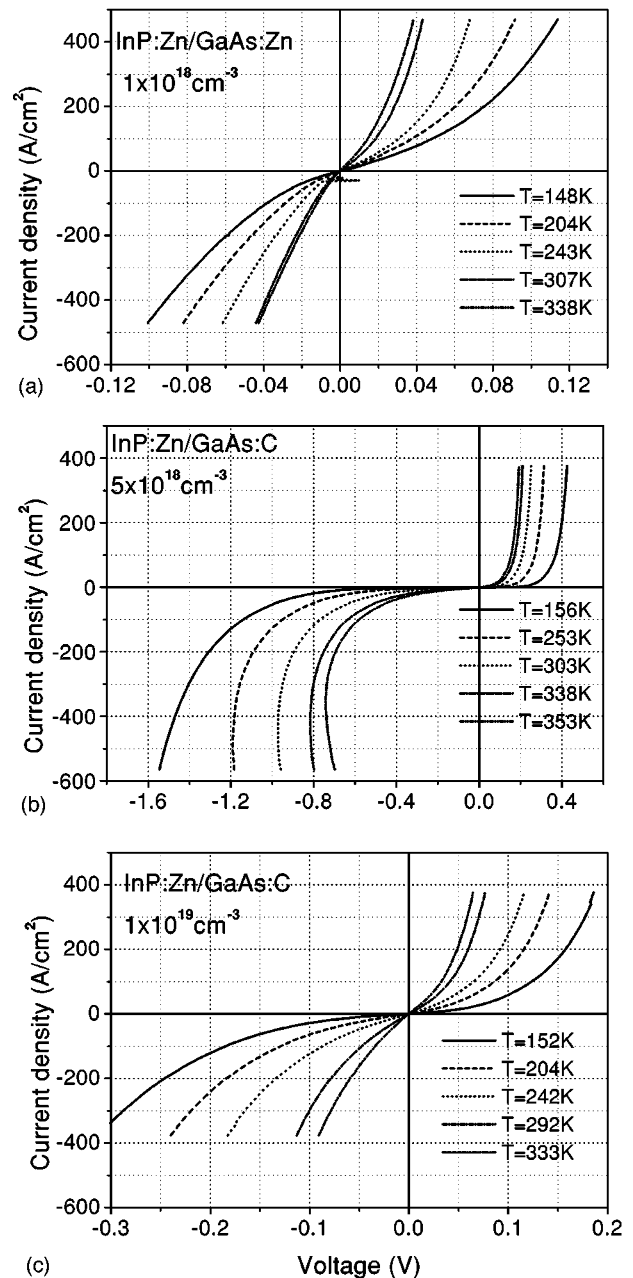

FIG. 7. Temperature dependent current voltage characteristics, (a) InP:Zn/GaAs:Zn, $p=1\times10^{18}$ cm^{-3}, (b) InP:Zn/GaAs:C, $p=5\times10^{18}$ cm^{-3}, (c) InP:Be/GaAs:C, $p=1\times10^{19}$ cm^{-3}.

THEORETICAL ANALYSIS

Measured current–voltage curves are simulated numerically using a standard one-dimensional semiconductor drift-diffusion model that includes Fermi statistics as well as thermionic emission and tunneling at heterobarriers.[31] To find agreement with the measurement, the GaAs/InP band offset and the interface charge density N_f are varied. Figure 8 shows the results of the fit to the measurements in Fig. 6(a). The band edge steps from InP to GaAs are found to be 0.05 eV in the valence band and 0.12 eV in the conduction band. These band offsets are used in the Richardson equation for thermionic emission and they are within the range expected from various models.[32] An increase of the band offsets gives an enhanced asymmetry of the current–voltage curves in Fig. 8. But the band offset alone does not result in the low current measured. An additional barrier within the valence band is required as formed by positive interface charges. The fitted charge density N_f is above 10^{12} cm^{-2} and it saturates at higher doping levels (Fig. 8). This interface charge behavior explains the surprising dependence of the results in Figs. 6(a) and 6(b) on the GaAs doping level. The nature of these charged defects as well as their interaction with acceptors is still unknown. The introduction of a single donor level at the interface does not give correct results in the simulation. Thus, several interacting energy levels are expected to be involved. The effect of temperature variation on the current–voltage curves (Fig. 7) can be simulated by a slight increase of N_f with rising temperature.

CONCLUSION

Record low voltage drops in the $I-V$ characteristics of wafer fused p-InP/p-GaAs heterojunctions were measured using zinc and carbon as doping elements in GaAs. When fused to InP:Zn, both dopants gave comparable electrical properties. The SIMS results showed an accumulation of Zn as well as C at the fused interface. Zn atoms are gettered at the interface when diffusing from the high doped InP side into GaAs. The concentration of accumulated Zn at the interface is sufficiently high to reduce the barrier in the valence band and the corresponding voltage drop in the $I-V$ characteristics. Carbon at the interface is believed to stem from the chemical treatment of the samples prior to fusion since no

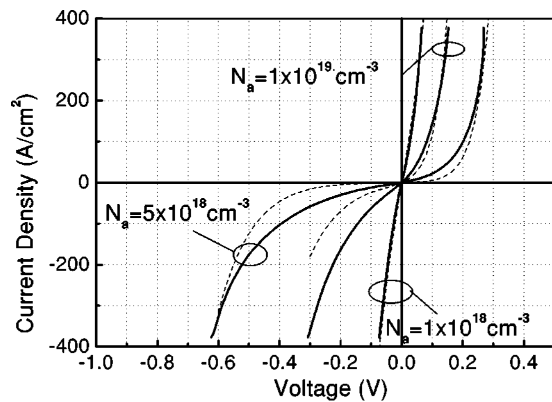

FIG. 8. Calculated current density vs voltage for different GaAs doping levels N_a: (a) $N_a=1\times10^{18}$ cm^{-3}, $N_f=2.6\times10^{12}$ cm^{-2}; (b) $N_a=5\times10^{18}$ cm^{-3}, $N_f=5.5\times10^{12}$ cm^{-2}; (c) $N_a=1\times10^{19}$ cm^{-3}, $N_f=5.5\times10^{12}$ cm^{-2} (N_f—positive interface charge density). Common parameters for all calculations: p-InP doping$=1e18$ cm^{-3}, 10 nm center Nd layer, $\Delta E_v=0.05$ eV, $\Delta E_c=0.12$ eV.

indications for C diffusion from GaAs to InP were found in the SIMS spectra. Although C is a p-type dopant in GaAs, it shows an amphoteric behavior in InP, which causes some difficulty to judge its role on the electrical properties. Since all samples showed low resistance and voltage drops, it is concluded that carbon in the measured concentration does not deteriorate the electrical behavior. SIMS measurements also revealed some oxygen at the fused interface. The area density of oxygen was 2.5×10^{14} cm^{-2}, which is not sufficient to form a continuous oxygen film between InP and GaAs.

The evaluation of the wafer fused interfaces that involved the InP:Be sample was complicated by large variations over the sample area. The Be concentration measured by SIMS in the bulk material as well as at the fused interface varied by a factor of two or more. Similar variations were found for electrical properties such as the voltage drop at reverse bias. From those findings, we conclude that low temperature grown InP, which can be produced by CBE or GSMBE, is not suitable for wafer fusion. This material degrades during the fusion process when it is exposed to high pressure and temperature. It is therefore very difficult to draw any conclusion on the role of Be on the electrical characteristics of wafer-fused heterojunctions. However, none of the samples in the InP:Be/GaAs series produced as low voltage drops or electrical resistance as the InP:Zn/GaAs samples. The indication that InP:Zn samples are more suitable for low resistive wafer fused interfaces than InP:Be could be related to the strong tendency of Zn to diffuse in InP and GaAs.[33]

The HRTEM results visualized the excellent crystalline quality of the fused junctions. The large lattice mismatch between GaAs and InP of 3.7% is accommodated by a set of edge dislocations with a dislocation spacing of 10 nm. Plan-view experiments revealed a 10° off-angle between the edge dislocations and the [110] direction caused by a slight misalignment between both samples. Although it is known, that the alignment between wafer fused samples can influence the electrical properties,[34] it is believed, that the measured twist angle of 0.5° is much too small to cause an increased electrical resistance. It is also worth noting that the results confirm that the wafer fusion process produces no or very few threading dislocations. Threading dislocations that are generated, e.g., by the metamorphic growth of GaAs on InP, degrade the optical properties of the material by scattering or diffraction. Furthermore their ability to propagate through the device structure can have severe implications on the reliability of, e.g., a VCSEL.

In the series of different GaAs doping levels, the lowest voltage drop in forward and reverse direction was reproducibly achieved with the lowest doping level of 1×10^{18} cm^{-3}. Increasing the acceptor concentration increased the voltage drop, which decreased again at even higher doping. This behavior was independent of the GaAs p dopant. The asymmetry in the $I-V$ curves in forward and reverse bias voltage could be modeled by assuming a positive charge density at the fused interface. In order to also describe the doping dependence, it was further assumed, that the interface charge increases with the acceptor concentration but saturates at about 5.5×10^{18} cm^{-3} at higher doping. The same model using a slightly increasing charge density with temperature could describe the temperature dependent $I-V$ curves. The nature of the charged interface defect is not known, but it is must be expected that it involves the interaction of several different energy states.

ACKNOWLEDGMENTS

We would like to thank M. Linnarsson for the SIMS measurements. The TEM work was performed at the Centre Interdepartemental de Microscopie Electronique (Ecole Polytechnique Federale de Lausanne). The financial support of the European ACTS:VERTICAL program and the Swedish National Board for Industrial and Technical Development (NUTEK) is also acknowledged.

[1] F. E. Ejeckam, C. L. Chua, Z. H. Zhu, Y. H. Lo, M. Hong, and R. Bhat, Appl. Phys. Lett. **67**, 3936 (1995).
[2] A. R. Hawkins, W. Wu, P. Abraham, K. Streubel, and J. E. Bowers, Appl. Phys. Lett. **70**, 303 (1997).
[3] J. J. Dudley, D. I. Babic, R. Mirin, L. Yang, B. I. Miller, R. J. Ram, T. Reynolds, E. L. Hu, and J. E. Bowers, Appl. Phys. Lett. **64**, 1463 (1994).
[4] D. I. Babic, J. J. Dudley, K. Streubel, R. P. Mirin, J. E. Bowers, and E. L. Hu, Appl. Phys. Lett. **66**, 1030 (1995).
[5] I.-H. Tan, J. J. Dudley, D. I. Babic, D. A. Coldren, B. D. Young, E. L. Hu, J. E. Bowers, B. I. Miller, U. Koren, and M. G. Young, IEEE Photonics Technol. Lett. **6**, 811 (1994).
[6] F. A. Kish, F. M. Steranka, D. C. DeFevere, D. A. Vanderwater, K. G. Park, C. P. Kuo, T. D. Osentowski, M. J. Peannasky, J. G. Yu, R. M. Fletcher, D. A. Steigwald, M. G. Craford, and V. M. Robbins, Appl. Phys. Lett. **64**, 2839 (1994).
[7] G. E. Hofler, D. A. Vanderwater, D. C. DeFevere, F. A. Kish, M. D. Camras, F. M. Steranka, and I.-H. Tan, Appl. Phys. Lett. **69**, 803 (1996).
[8] Z. L. Liua, J. N. Walpole, and D. Z. Tsang, IEEE J. Quantum Electron. **QE-20**, 855 (1984).
[9] Y. H. Lo, R. Bhat, D. M. Hwang, M. A. Koza, and T. P. Lee, Appl. Phys. Lett. **58**, 1961 (1991).
[10] K. Miro, K. Tokutome, K. Nishi, and S. Sugou, Electron. Lett. **30**, 1008 (1994).
[11] A. V. Syrbu, J. Fernandez, J. Behrend, C. A. Berseth, J. F. Carlin, A. Rudra, and E. Kapon, Electron. Lett. **33**, 866 (1997).
[12] D. I. Babic, K. Streubel, R. P. Mirin, N. M. Margalit, J. E. Bowers, E. L. Hu, D. E. Mars, L. Yang, and K. Carey, IEEE Photonics Technol. Lett. **7**, 1225 (1995).

[13] Y. Ohiso, C. Amano, Y. Itoh, K. Tateno, T. Tadokoro, H. Takenouchi, and T. Kurokawa, Electron. Lett. **32**, 1483 (1996).
[14] N. M. Margalit, D. I. Babic, K. Streubel, R. P. Mirin, R. L. Naone, J. E. Bowers, and E. L. Hu, Electron. Lett. **32**, 1675 (1996).
[15] S. Rapp, J. Piprek, K. Streubel, J. André, E. Rodriguez Messmer, and J. Wallin, Temperature performance of 1.55-μm-vertical cavity lasers with integrated InP/GaInAsP Bragg reflector, IPRM, Hyanis, 1997.
[16] H. Wada, Y. Ogawa, and T. Kamijoh, Appl. Phys. Lett. **62**, 738 (1993).
[17] R. J. Ram, J. J. Dudley, J. E. Bowers, L. Yang, K. Carey, S. J. Rosner, and K. Nauka, J. Appl. Phys. **78**, 4227 (1995).
[18] C. H. Henry, A. Logan, F. R. Merrit, and J. P. Luongo, IEEE J. Quantum Electron. **QE-19**, 947 (1983).
[19] D. I. Babic, Ph.D. dissertation, University of California, Santa Barbara, 1995.
[20] E. F. Schubert, C. J. Pinzond, and M. Geva, Appl. Phys. Lett. **67**, 700 (1995).
[21] E. Veuhoff, H. Baumeister, J. Rieger, M. Gorgel, and R. Treichler, J. Electron. Mater. **20**, 1037 (1991).
[22] E. Kuphal, Solid-State Electron. **24**, 69 (1980).
[23] N. Kobayashi, T. Makimoto, and Y. Horikoshi, Appl. Phys. Lett. **50**, 1435 (1987).
[24] B. T. Cunningham, L. J. Guido, J. E. Baker, J. S. Major Jr., N. Holonyak Jr., and G. E. Stillman, J. Appl. Phys. Lett. **55**, 687 (1989).
[25] E. F. Schubert, *Doping in III–V Semiconductors* (Cambridge University Press, Cambridge, 1993).
[26] M. Ilegems and W. C. O'Mara, J. Appl. Phys. **43**, 1190 (1972).
[27] D. Ritter, R. A. Hamm, M. B. Panish, and M. Geva, Appl. Phys. Lett. **63**, 1543 (1993).
[28] W. T. Tsang, B. Tell, J. A. Ditzenberger, and A. H. Dayem, J. Appl. Phys. **60**, 4182 (1986).
[29] L. Sagalowicz, A. Rudra, A. Sirbu, J. Behrend, F. Salomonson, K. Streubel, M. Hammar, and E. Kapon, Philos. Mag. Lett. (to be published).
[30] A. Rudra (unpublished).
[31] Sim Windows32 by D. W. Winston, University of Colorado, Bolder (1996).
[32] *Heterojunction Band Discontinuities*, edited by F. Capasso and G. Margaritondo (North-Holland, Amsterdam, 1987).
[33] J. Jaquet, P. Salet, A. Plais, F. Brillouet, E. Derouin, L. Goldstein, C. Fortin, F. Gaborit, P. Pagnod, H. Bissessur, J-L. Lafragette, F. Gerard, J. Pasquier, and S. Starck, J. Phys. (France) (to be published).
[34] F. A. Kish, D. A. Vanderwater, M. J. Peanasky, M. J. Ludowse, S. G. Hummel, and S. J. Rosner, Appl. Phys. Lett. **67**, 2060 (1995).